IEICE TRANS. COMMUN., VOL.E103–B, NO.9 SEPTEMBER 2020

PAPER

Performance Evaluation of IDMA-Based Random Access with Various Structures of Interference Canceller*

Masayuki KAWATA[†], **Kiichi TATEISHI**[††], ***Nonmembers***, ***and*** **Kenichi HIGUCHI**[†a)], ***Senior Member***

SUMMARY This paper investigates the performance of interleave division multiple access (IDMA)-based random access with various interference canceller structures in order to support massive machine-type communications (mMTC) in the fifth generation (5G) mobile communication system. To support massive connectivity in the uplink, a grant-free and contention-based multiple access scheme is essential to reduce the control signaling overhead and transmission latency. To suppress the packet loss due to collision and to achieve multi-packet reception, non-orthogonal multiple access (NOMA) with interference cancellation at the base station receiver is essential. We use IDMA and compare various interference canceller structures such as the parallel interference canceller (PIC), successive interference canceller (SIC), and their hybrid from the viewpoints of the error rate and decoding delay time. Based on extensive computer simulations, we show that IDMA-based random access is a promising scheme for supporting mMTC and the PIC-SIC hybrid achieves a good tradeoff between the error rate and decoding delay time.

key words: *IDMA, random access, mMTC, interference canceller, PIC, SIC*

1. Introduction

In the fifth-generation (5G) mobile communication system [1]–[3], massive machine-type communications (mMTC) will be supported to actualize the Internet-of-Things (IoT) in which a massive number of terminals (hereafter we denote this general term of 'terminal' as 'user' for simplicity) sends small data packets to a base station. In LTE and LTE-Advanced [4], [5], scheduling-based orthogonal packet access based on single carrier – frequency division multiple access (SC-FDMA) is employed in the uplink. SC-FDMA can remove inter-user interference within a cell, i.e., avoid packet collision, and achieve a multiuser diversity gain via channel-aware scheduling. However, as the number of users increases, the control-signaling overhead and transmission delay increase. Therefore, to support uplink mMTC, a grant-free and contention-based multiple access scheme is essential to reduce the control signaling overhead and transmission latency. To suppress the packet loss due to collision and to achieve multi-packet reception [6], non-orthogonal multiple access (NOMA) with interference cancellation at the base station receiver is essential.

Recently, NOMA has gained more attention as a candidate multiple access scheme for future radio access [7]–[12]. In the downlink, NOMA referred to as downlink Multi-User Superposition Transmission (MUST) has already been incorporated into LTE-Advanced [13] targeting further enhancement of mobile broadband.

To enhance the performance of cellular uplink, i.e., multiple-access channel, various proposals have been made, interleave division multiple access (IDMA) [14], [15], low density signature (LDS) [16], and sparse code multiple access (SCMA) [17], [18] etc., which are categorized into NOMA. Among these, LDS and SCMA are characterized as having a sparse transmission signal format and can reduce the inter-packet interference at the base station receiver with low computational complexity by using a message-passing algorithm (MPA). However, LDS and SCMA and their variants may require tight time/frequency synchronization among users and cause high peak power on the user terminal transmitter side due to the nature of the sparse signal transmission. In an uplink mMTC scenario, these drawbacks may not be acceptable; therefore, we take the IDMA-based approach in this paper.

In IDMA, multiple packets transmitted simultaneously from different terminals are decomposed by multiuser detection at the base station receiver in which user-specific channel interleavers are utilized. The IDMA signal does not increase the peak power and its transmission performance is robust against the error in time/frequency synchronization among users. These are desirable properties in uplink mMTC.

The transmission performance of IDMA-based random access is largely dependent on the structure of the interference canceller receiver. Therefore, this paper investigates various interference canceller structures appropriate for IDMA-based random access. We note that the contents of this paper are based on [19], but include enhanced evaluation and discussions. We compare the parallel interference canceller (PIC), successive interference canceller (SIC), and their hybrid from the viewpoints of the error rate and decoding delay time. Although these interference canceller structures studied in this paper are existing ones, e.g., in [20]–[23], there are no detailed comparative evaluations of these interference canceller structures considering their application to random access based on IDMA, which is the main contribution and novelty of this work. We assume frequency-domain

Manuscript received October 21, 2019.
Manuscript revised February 23, 2020.
Manuscript publicized March 23, 2020.

[†]The authors are with the Department of Electrical Engineering, Graduate School of Science and Technology, Tokyo University of Science, Noda-shi, 278-8510 Japan.
[††]The author is with Radio Access Network Development Department, NTT DOCOMO, INC, Yokosuka-shi, 239-8536 Japan.

*The material in this paper was presented in part at the IEEE 88th Vehicular Technology Conference, Chicago, U.S.A., August 2018.

a) E-mail: higuchik@rs.tus.ac.jp

DOI: 10.1587/transcom.2019EBP3220

signal processing for all interference cancellers in this paper. Based on extensive computer simulations, we show that IDMA-based random access is a promising scheme for supporting mMTC and the PIC-SIC hybrid achieves a good tradeoff between the error rate and decoding delay time.

We also present a performance comparison of IDMA-based random access with orthogonal multiple access (OMA)-like random access from the viewpoint of supporting mMTC in the 5G system. We show that IDMA-based random access achieves much better transmission performance than OMA-like random access. This is thanks to its greater frequency diversity gain, use of lower coding rates, reduced variation in the number of simultaneously transmitted packets per channel, and its total interference power normalized by the channel coding rate due to the enhanced statistical multiplexing effect obtained from the wider transmission bandwidth.

The remainder of the paper is organized as follows. First, Sect. 2 describes IDMA-based random access and the basic interference cancelling process. Section 3 presents the three evaluated interference canceller structures. Section 4 presents numerical results based on computer simulations. Finally, Sect. 5 concludes the paper.

2. IDMA-Based Random Access and Basic Interference Cancelling Process

Figure 1 shows the IDMA-based random access procedure. The base station periodically broadcasts a set of available channel interleaver patterns via the downlink. The user terminals having uplink information to be transmitted randomly select one channel interleaver from the informed set. They then generate packets using the selected channel interleaver and transmit the packets. Finally, the base station decodes the received packets using the interference canceller and feeds back ACK information to the user terminals whose packets are correctly decoded.

In the following, we assume a set of users, $\mathcal{K}$, transmits packets simultaneously. Here, $|\mathcal{K}|$ is denoted as K. At each transmitter, the transmission information bit sequence is processed with turbo coding and repetition coding. The coded bit sequence is channel interleaved and data symbol mapping is applied. We assume QPSK data modulation in the paper and P_{d} denotes the symbol power. We assume a single-carrier transmission and the data symbol sequence is block-wised (hereafter denoted as discrete Fourier transform (DFT)-block) with the block size of N. We denote the $N \times 1$-dimensional time-domain DFT-block data symbol vector of user $k \in \mathcal{K}$ as $\mathbf{x}_k = [x_{k,1}, \ldots, x_{k,N}]^T$, where $x_{k,n}$ ($n = 1, \ldots, N$) is the n-th QPSK modulated data symbol. We assume a single transmitter antenna per user in the paper.

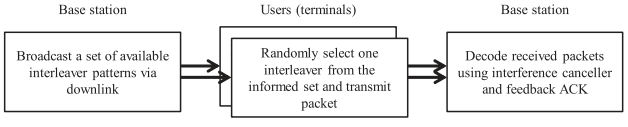

Fig. 1 IDMA-based random access scheme.

We assume L receiver antennas at the base station in the paper. We also assume that a cyclic prefix (CP) is appended to each DFT block [24], [25] in the single-carrier transmission and the CP length is sufficiently long so that it covers the entire multipath delay spread and the difference in the received signal timings among users. The $N \times N$-dimensional time domain channel matrix, $\mathbf{G}_k^{(l)}$, of user k at receiver antenna l ($l = 1, \ldots, L$) can be represented as

$$\mathbf{G}_k^{(l)} = \mathbf{F}^H \mathrm{diag}_n\{H_{k,n}^{(l)}\}\mathbf{F}, \tag{1}$$

where $\mathbf{F}$ is the $N \times N$-dimensional DFT matrix assuming $\mathbf{F}^H\mathbf{F} = \mathbf{F}\mathbf{F}^H = \mathbf{I}$ and $H_{k,n}^{(l)}$ is the channel frequency response of user k at frequency n at receiver antenna l.

Therefore, denoting the frequency domain transmitted signal component of user k at frequency n as $X_{k,n}$, which corresponds to the n-th element of $\mathbf{F}\mathbf{x}_k$, the frequency domain received signal at frequency n at receiver antenna l, $Y_n^{(l)}$, is represented as

$$Y_n^{(l)} = \sum_{k \in \mathcal{K}} H_{k,n}^{(l)} X_{k,n} + Z_n^{(l)}, \tag{2}$$

where $Z_n^{(l)}$ represents the i.i.d. additive white Gaussian noise (AWGN) term at frequency n at receiver antenna l with power N_0.

In this paper, we assume a computationally efficient frequency-domain interference cancelling process. First, antenna diversity combining is performed. We use maximum ratio combining (MRC) in the paper to reduce the complexity. The combined received signal at frequency n for user k is represented as

$$\tilde{Y}_n^{[k]} = \frac{1}{\sqrt{\sum_{l=1}^{L} |H_{k,n}^{(l)}|^2}} \sum_{l=1}^{L} H_{k,n}^{(l),*} Y_n^{(l)}, \tag{3}$$

where the effective channel of user u in $\tilde{Y}_n^{[k]}$, $\tilde{H}_{u,n}^{[k]}$, is represented as

$$\tilde{H}_{u,n}^{[k]} = \frac{1}{\sqrt{\sum_{l=1}^{L} |H_{k,n}^{(l)}|^2}} \sum_{l=1}^{L} H_{k,n}^{(l),*} H_{u,n}^{(l)}. \tag{4}$$

The interference cancellation is processed by alternately performing minimum mean squared error (MMSE)-based symbol estimation (estimation of $\{\mathbf{x}_k\}$) and channel decoding. In the MMSE-based symbol estimation, the channel decoding results are used as *a priori* information that achieves a soft-decision interference canceller.

Based on [26], the MMSE-based symbol estimator outputs the estimate of $\mathbf{x}_k$, $\hat{\mathbf{x}}_k$, as

$$\hat{\mathbf{x}}_k = \mathbf{F}^H \begin{bmatrix} \vdots \\ \dfrac{W_k \tilde{H}_{k,n}^{[k],*}}{\sum_{u\in\mathcal{K}} \bar{v}_u |\tilde{H}_{u,n}^{[k]}|^2 + N_0} \left(\tilde{Y}_n^{[k]} - \sum_{u\in\mathcal{K}} \tilde{H}_{u,n}^{[k]} \bar{X}_{u,n} \right) \\ + \left(\dfrac{W_k}{N} \sum_{n=1}^{N} \dfrac{|\tilde{H}_{k,n}^{[k]}|^2}{\sum_{u\in\mathcal{K}} \bar{v}_u |\tilde{H}_{u,n}^{[k]}|^2 + N_0} \right) \bar{X}_{k,n} \\ \vdots \end{bmatrix}, \tag{5}$$

where

$$W_k = \frac{P_{\mathrm{d}}}{\dfrac{P_{\mathrm{d}} - \bar{v}_k}{N} \sum_{n=1}^{N} \dfrac{|\tilde{H}_{k,n}^{[k]}|^2}{\sum_{u\in\mathcal{K}} \bar{v}_u |\tilde{H}_{u,n}^{[k]}|^2 + N_0} + 1}. \tag{6}$$

In (5) and (6),

$$\begin{aligned} \left[\bar{X}_{k,1} \quad \cdots \quad \bar{X}_{k,N} \right]^T &= \mathbf{F} \left[\mathrm{E}[x_{k,1}] \quad \cdots \quad \mathrm{E}[x_{k,N}] \right]^T \\ \bar{v}_k &= \frac{1}{N} \sum\nolimits_{n=1}^{N} \mathrm{Var}[x_{k,n}] \end{aligned}, \tag{7}$$

and $\mathrm{E}[x_{k,n}]$ and $\mathrm{Var}[x_{k,n}]$ are calculated from the log-likelihood ratio (LLR) of coded bits constructing $x_{k,n}$ from the previous channel decoding results as *a priori* information [27].

Based on $\hat{\mathbf{x}}_k$, the LLR of the coded bits of user k is calculated as an output of the MMSE-based symbol estimator and is input to the channel decoder. We assume for simplicity that the MMSE-based symbol estimate, $\hat{\mathbf{x}}_k$, derived using (5) is approximated as the output of the Gaussian channel to calculate the LLR of the coded bits. By repeating the above process, the inter-user interference and the inter-symbol interference due to the multipath channel are suppressed.

We note that in a real system, error detection coding such as cyclic redundancy check (CRC) coding is applied in addition to the error correction coding. In this paper, we assume that after channel decoding, if there is no channel decoding error in the user k packet, hard-decision interference cancellation based on the decoding results is applied to that packet instead of soft-decision interference cancellation in (5) to reduce the computational cost and improve the error rate.

3. Evaluated Interference Cancellers

In this paper, from the viewpoints of the error rate and decoding delay time, we comparatively study three interference canceller structures appropriate for IDMA-based random access: the PIC, SIC, and PIC-SIC hybrid. Figures 2(a)–2(c) are block diagrams of the respective interference cancellers.

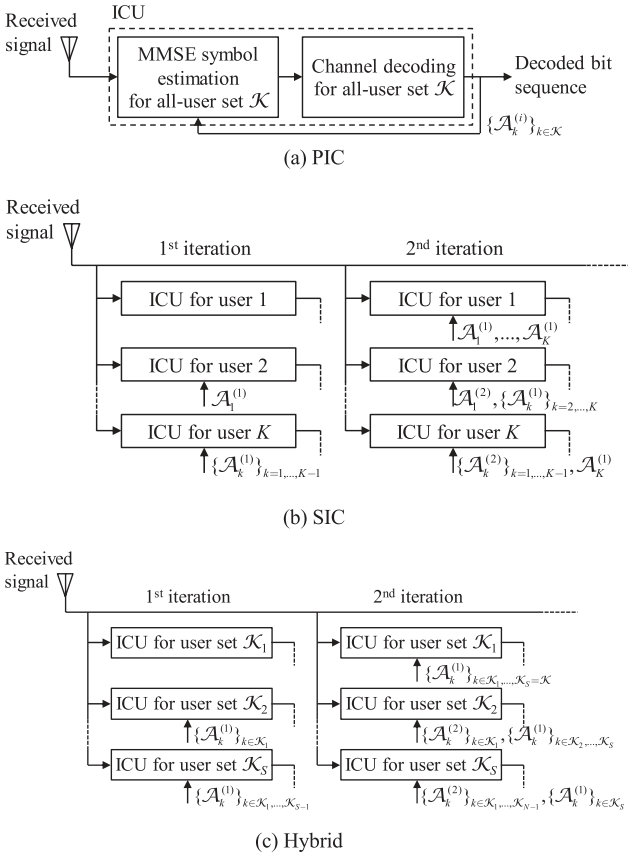

Fig. 2 Block diagrams of evaluated interference cancellers.

3.1 PIC

As described in Sect. 2, the interference canceller comprises the MMSE-based symbol estimator and channel decoder. This set is called the interference cancellation unit (ICU) hereafter. The interference canceler repeats the ICU process for a given number of iterations. In the PIC, the ICU processes all-user set $\mathcal{K}$ simultaneously in the ICU. At the i-th iteration, the MMSE-based symbol estimator utilizes the channel decoding results of all users at the $i-1$-th iteration as *a priori* information. The set of *a priori* information (corresponds to the set of information in (7)) of user k obtained from the i-th channel decoding of that user is denoted as $\mathcal{A}_k^{(i)}$. Since the PIC processes all users simultaneously, at the i-th iterative process of ICU, $\{\mathcal{A}_k^{(i-1)}\}_{k\in\mathcal{K}}$ are used as *a priori* information and $\{\mathcal{A}_k^{(i)}\}_{k\in\mathcal{K}}$ is output. The advantageous property of the PIC is its short processing delay. However, since the received signal power of the respective users may be different due to channel fading, simultaneous processing may result in inaccurate decoding results, which may lead to an increased error rate and/or increased total number of decoding processes (calculation complexity).

3.2 SIC

In order to improve the decoding accuracy per ICU process, the SIC is evaluated. As shown in Fig. 2(b), the SIC sequentially decodes the received signal user-by-user within the iterative process. In this paper, we assume that the users are sorted based on the received signal power after antenna diversity reception, and decoding is started from the user with the highest received signal power. In the ICU of user k at the i-th iteration, *a priori* information of users $1 \sim k-1$ obtained from the decoder outputs in the i-th iteration, $\{\mathcal{A}_u^{(i)}\}_{u=1,\ldots,k-1}$, and that of users $k \sim K$ obtained from the decoder outputs in the $i-1$-th iteration, $\{\mathcal{A}_u^{(i-1)}\}_{u=k,\ldots,K}$, are utilized. By using more recent decoding results from users whose received power is higher than that user, the error rate is expected to be lower than that of the PIC. The drawback to the SIC is its longer processing delay due to the serial signal processing compared to the PIC.

3.3 PIC-SIC Hybrid

In order to reduce the processing delay in the SIC, in other words, to achieve a good performance tradeoff between the PIC and SIC, we investigate a PIC-SIC hybrid method as shown in Fig. 2(c). In the hybrid method, the overall user set $\mathcal{K}$ is divided into S subsets, $\mathcal{K}_1, \ldots, \mathcal{K}_S$. Within user subset $\mathcal{K}_s$ ($s = 1, \ldots, S$), parallel processing is applied, while between different user subsets, serial processing is applied. Thus, in the ICU of user subset $\mathcal{K}_s$ at the i-th iteration, *a priori* information of user subsets $\mathcal{K}_1 \sim \mathcal{K}_{s-1}$ obtained from the decoder outputs in the i-th iteration, $\{\mathcal{A}_u^{(i)}\}_{u\in\mathcal{K}_1,\ldots,\mathcal{K}_{s-1}}$, and that of users $\mathcal{K}_s \sim \mathcal{K}_S$ obtained from the decoder outputs in the $i-1$-th iteration, $\{\mathcal{A}_u^{(i-1)}\}_{u\in\mathcal{K}_s,\ldots,\mathcal{K}_S}$, are utilized.

4. Numerical Results

Table 1 gives the simulation parameters. We assume DFT-spread OFDM-based single-carrier transmission [25]. The number of information bits per packet is 106. The number of subcarriers (= DFT size) is 240 with the subcarrier spacing of 15 kHz, which corresponds to a 3.6-MHz transmission bandwidth. One packet comprises 7 DFT blocks and the packet length is 0.5 ms including the CP. As channel coding, we use the combination of the turbo code and repetition code. The turbo code with the mother code rate of 1/3 and the constraint length of 4, which is used in the 3GPP [25], is applied (its generator polynomials are 13, 15, and 15 in octal notation). The number of repetitions in the repetition coding is set to 10. QPSK data modulation is assumed. A random interleaver is used as a channel interleaver.

The user arrival for each 0.5-ms packet slot per 3.6 MHz is Poisson distributed with the mean of λ users, where λ is parameterized in the following evaluation. As the frequency selective fading channel model, we assume block Rayleigh fading with an exponentially decayed 6-path model where the rms delay spread is set to 1 μs. Here, L = 4-branch receiver antenna diversity is employed. The Max-Log MAP (maximum *a posteriori*) decoding with eight iterations is used to decode the turbo code. The maximum number of iterations in the interference cancellation, J, is parameterized. In the PIC-SIC hybrid method, the number of users per subgroup, K_{sub}, is parameterized.

Table 1 Simulation parameters.

Number of information bits		106
Transmission bandwidth		3.6 MHz
Number of subcarriers		240 (15-kHz subcarrier spacing)
Packet length		0.5 ms = 7 DFT blocks
Channel coding	Turbo code	Mother code: Rate-1/3 turbo code (k = 4), Max-Log MAP decoding (8 iterations)
	Repetition code	10 repetitions
Data modulation		QPSK
User arrival		Poisson distributed with mean of λ users per 0.5-ms packet slot per 3.6 MHz
Channel model		Six-path block Rayleigh, rms delay spread = 1 μs
Antenna diversity reception		L = 4-branch maximum ratio combining
Maximum number of iterations in interference cancellation		J
Number of users per subgroup in hybrid method		K_{sub}

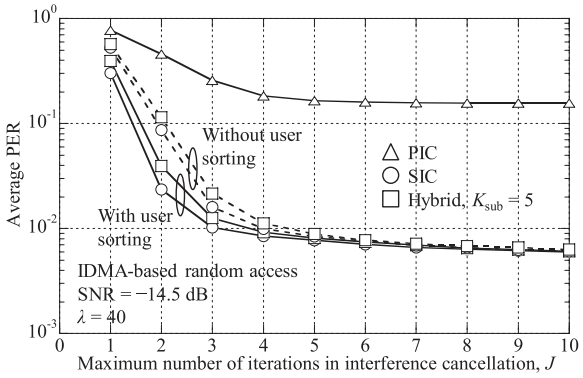

Fig. 3 Average PER as a function of maximum number of iterations, J.

We also evaluated the case corresponding to OMA-like random access, where multiple frequency blocks are prepared for a random access channel, for comparison with IDMA-based random access. In the OMA scenario, the number of subcarriers per frequency block is set to 24 and no repetition is applied to convey the same 106 information bits. The user arrival rate within a 24-subcarrier (= 0.36-MHz) unit bandwidth in the OMA case is reduced to 1/10 of the IDMA case, assuming that there are 10 frequency blocks (in total 240 subcarriers) for the random access channel in the OMA scenario. In the OMA scenario, we assume the same PIC receiver structure as in the IDMA scenario, in order to resolve the packet collision as much as possible.

Figure 3 shows the average packet error rate (PER) as a function of the maximum number of iterations in interference cancellation, J. The signal-to-noise ratio (SNR) is set to −14.5 dB considering the target PER of 10^{-2}. User arrival rate λ is set to 40. Three interference canceller structures,

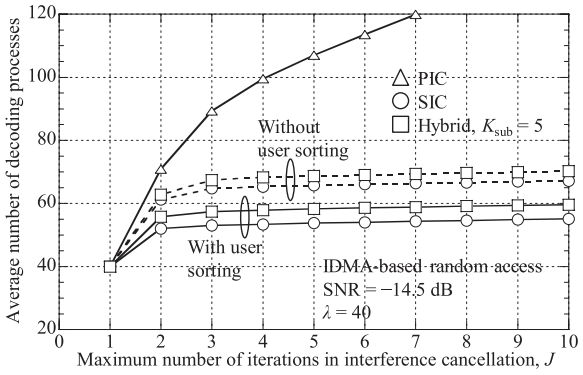

Fig. 4 Average number of decoding processes as a function of maximum number of iterations, J.

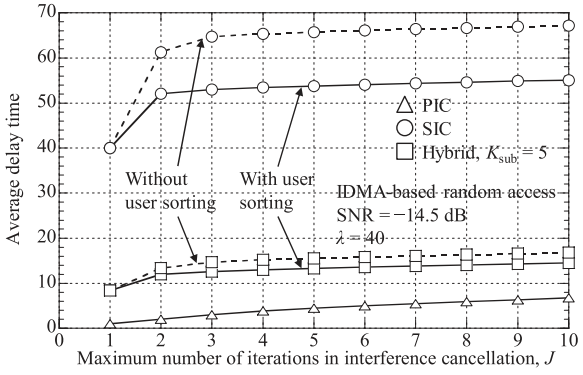

Fig. 5 Average delay time as a function of maximum number of iterations, J.

PIC, SIC, and hybrid method with K_{sub} of 5 are evaluated for comparison. In the SIC and hybrid methods, two cases with and without user sorting based on the received signal power after antenna diversity reception are tested. In all interference cancellers, the PER decreases as J is increased due to more accurate inter-user interference cancellation. The effectiveness of the user sorting in SIC and hybrid methods is confirmed from Fig. 3. The use of user sorting in the SIC and hybrid methods is especially effective when J is limited, since the accuracy in inter-user interference cancellation per iteration is improved.

Figures 4 and 5 show the average number of decoding processes and delay time, respectively, as a function of J. The SNR is set to -14.5 dB. Here, λ is set to 40. The delay time is defined as the number of serially performed ICU processes. In all interference cancellers, the average number of decoding processes and delay time increase as J is increased because the decoder tries to achieve more accurate decoding by repeating the ICU process. Both the SIC and hybrid method with user sorting reduce the average number of decoding processes and delay time compared to the cases without user sorting due to more efficient use of decoding results.

From the perspective of decoding accuracy, computational complexity and decoding delay time, it is important to sort users so that the SIC and hybrid method achieve better

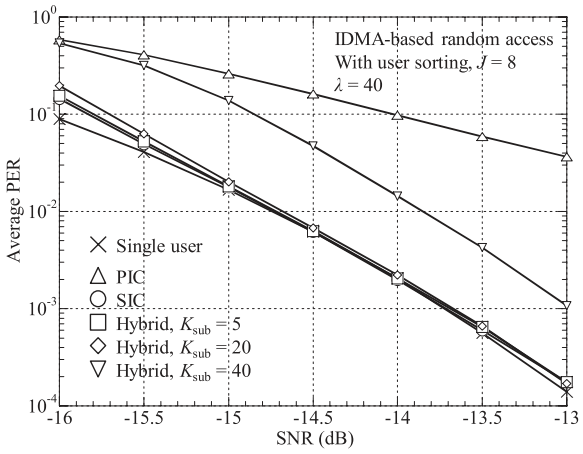

Fig. 6 Average PER as a function of SNR.

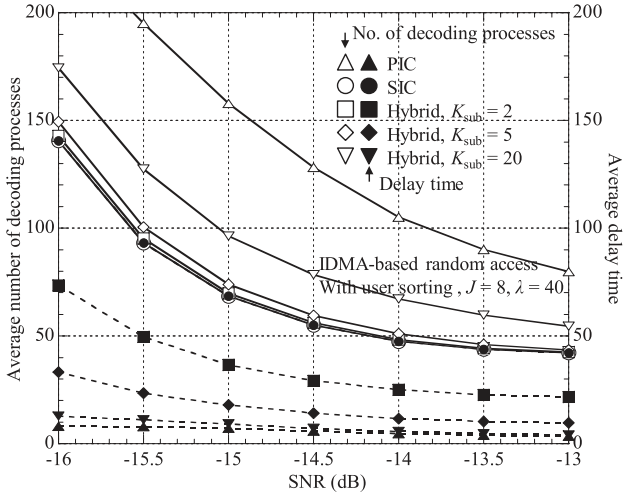

Fig. 7 Average number of decoding processes and delay time as a function of SNR.

performance. In the following evaluations, in the SIC and hybrid method, users are sorted based on the received signal power after antenna diversity reception, and decoding is started from the user with the highest received signal power. Furthermore, J is set to 8 in the following evaluations because the additional gain in the PER by increasing J further beyond 8 is marginal.

Figure 6 shows the average PER as a function of the SNR where the number of users per subgroup, K_{sub}, is parameterized in the hybrid method. Here, λ is set to 40. As a reference, the PER in a single user case is also plotted. The SIC reduces the PER significantly compared to the PIC due to more accurate interference cancellation. Furthermore, the hybrid method achieves quite comparable PER performance with the SIC method. Interestingly, the performance of the hybrid method is rather robust against the K_{sub} value. Only when K_{sub} is set very high such as 40, clear PER performance degradation is observed.

Figure 7 shows the average number of decoding processes and delay time as a function of the SNR for the various

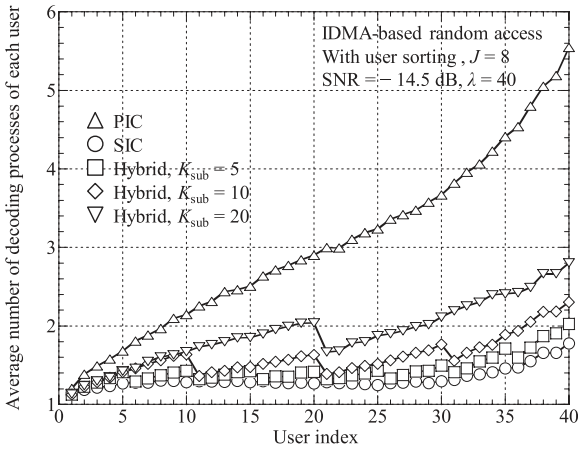

Fig. 8 Average number of decoding processes of each user as a function of user index.

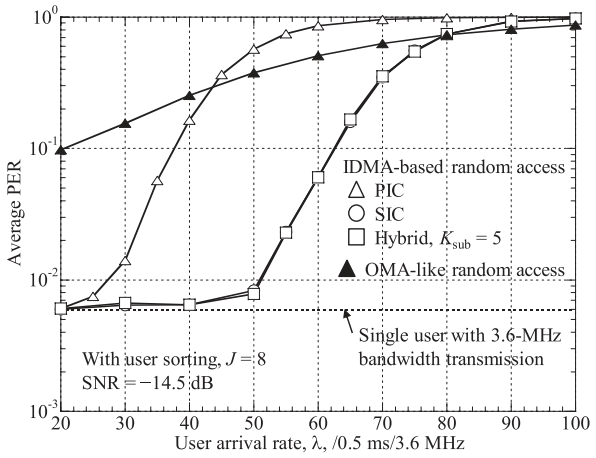

Fig. 9 Average PER as a function of user arrival rate, λ.

interference canceller structures. Here, λ is set to 40. The SIC and hybrid methods largely reduce the number of decoding processes compared to the PIC, thanks to the improved accuracy in the interference cancellation per ICU process. However, the decoding processing delay time of the SIC is longest among the three interference cancellers, although its number of decoding processes is the lowest. Meanwhile, the hybrid method achieves approximately the same PER and number of decoding processes as the SIC, and the delay time is effectively reduced to levels comparable to that with the PIC. In the hybrid method, the choice of K_{sub} can control the tradeoff relationship between the number of decoding processes and delay time.

Figure 8 shows the average number of decoding processes of each user as a function of the user index. The user index is sorted in decreasing order of the received signal power after antenna diversity reception of the respective users. The SNR is set to −14.5 dB. User arrival rate λ is set to 40. This figure confirms that the SIC and hybrid methods reduce the number of decoding processes of every user compared to the PIC.

Figure 9 shows the average PER as a function of the user arrival rate, λ. The SNR is set to −14.5 dB and K_{sub} of the hybrid method is set to 5. For comparison, the performance levels with the OMA-like random access are also plotted. The SNR in the OMA scenario is set 10-dB higher to compensate for the 1/10 transmission bandwidth reduction for fair comparison. Single user performance is also shown as a reference, which is not a function of λ on the horizontal axis.

First, the PER of the IDMA-based random access is significantly improved compared to the OMA-like random access. To explain the reasons behind this performance improvement, Figs. 10(a) and 10(b) show the average PER as a function of the number of users simultaneously transmitting the packet using the same channel and the cumulative probability of that when Poisson arrival with λ of 40 is assumed for IDMA-based and OMA-like random access, respectively. In the case of OMA-like random access, since

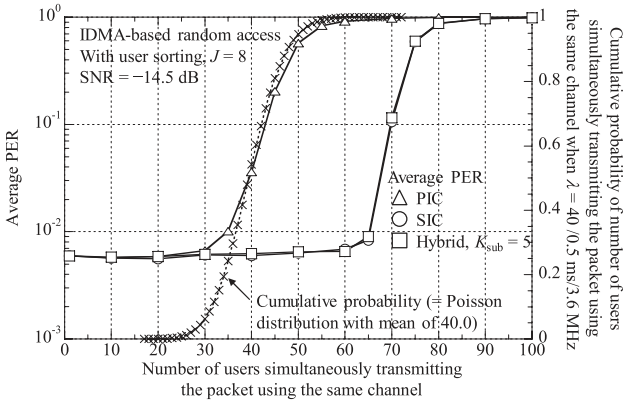

(a) IDMA-based random access

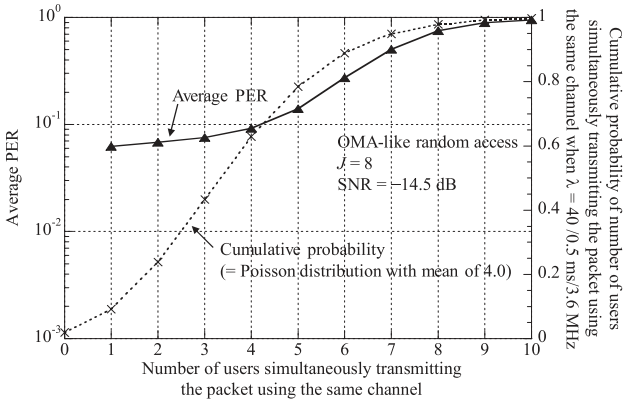

(b) OMA-like random access

Fig. 10 Average PER as a function of number of users simultaneously transmitting the packet using the same channel and its cumulative probability when Poisson user arrival with λ of 40 is assumed.

there are 10 frequency blocks, the cumulative probability of the number of users simultaneously transmitting the packet using the same channel follows a Poisson distribution with the mean of $\lambda/10 = 4$. Figures 10(a) and 10(b) show several advantageous properties of IDMA-based random access

that contribute to the performance improvement observed in Fig. 9. First, the PER in single user transmission with the full 3.6-MHz transmission bandwidth assumed in IDMA-based random access is lower than that with the 1/10-fold transmission bandwidth assumed in OMA-like random access with 10 frequency blocks. This is due to the lower channel coding rate (in this paper, we decrease the repetition coding rate) and greater frequency diversity in a frequency-selective channel due to multipaths. The second reason is the enhanced statistical multiplexing effect obtained from the wider transmission bandwidth per packet with regard to the variations in interference power and the number of interfering users. To achieve multi-packet reception in random access by resolving packet collisions using the interference canceller, the total interference power and number of users simultaneously transmitting the packet using the same channel should be within the allowable limits for correct packet decoding. Since these allowable limits are roughly proportional to the number of repetitions in the repetition code, they should be normalized by the number of repetitions for comparison purposes. From Figs. 10(a) and 10(b), IDMA-based random access exhibits a steep change in PER with respect to the number of users simultaneously transmitting the packet normalized by the number of repetitions, and fluctuates in a narrower range of the normalized number of users simultaneously transmitting the packet than OMA-like random access. This is because although the interference power (thus, received signal power) of each user fluctuates due to fading, the variation in the normalized total interference power becomes small in IDMA-based random access due to the averaging effect among users since the total number of interfering users is large. Furthermore, IDMA-based random access reduces the variation in the number of users simultaneously transmitting the packet using the same channel normalized by the number of repetitions compared to OMA-like random access assuming the same Poisson user arrival rate, λ, for the entire transmission bandwidth for random access. This is also thanks to the enhanced statistical multiplexing effect. These properties of IDMA-based random access are desirable to perform accurate and stable interference cancellation to resolve packet collisions.

When comparing the three interference canceller structures for IDMA-based random access, the performance of the PIC is largely degraded as λ increases compared to the SIC and hybrid methods. When λ is equal to or less than 50, the PER levels of the SIC and hybrid methods are robust against the increase in λ and good PER performance which is very close to that in the single user scenario is maintained. Considering also the number of decoding processes and delay time, the IDMA-based random access scheme utilizing the PIC-SIC hybrid interference canceller is a promising approach.

5. Conclusion

This paper investigated various interference canceller structures appropriate for the IDMA-based random access scheme and presented a performance comparison with OMA-like random access from the viewpoint of supporting mMTC in the 5G system. We showed that IDMA-based random access achieves much better transmission performance than OMA-like random access. This is thanks to its greater frequency diversity gain, use of lower coding rates, reduced variation in the normalized number of simultaneously transmitted packets per channel, and its total interference power due to the enhanced statistical multiplexing effect obtained from the wider transmission bandwidth. We also showed that the PIC-SIC hybrid interference canceller is a promising approach to achieve a good tradeoff between the achievable PER, number of decoding processes, and decoding delay time. As for future issues to be investigated, we will study the user identification and channel estimation issues, hybrid automatic repeat request (ARQ) protocol, and transmission power control [28] appropriate for IDMA-based random access.

References

[1] ITU-R, “IMT Vision - Framework and overall objectives of the future development of IMT for 2020 and beyond,” Recommendation M.2083-0, Sept. 2015.
[2] 3GPP TR38.913 (V0.4.0), “Study on scenarios and requirements for next generation access technologies (Release 14),” June 2016.
[3] 3GPP TR38.912 (V0.0.1), “Study on new radio access technology (Release 14),” June 2016.
[4] 3GPP TR36.913 (V8.0.0), “Requirements for further advancements for E-UTRA (LTE-Advanced),” June 2008.
[5] 3GPP TR36.814 (V9.0.0), “Further advancements for E-UTRA physical layer aspects,” March 2010.
[6] J. Metzner, “On improving utilization in ALOHA networks,” IEEE Trans. Commun., vol.COM-24, no.4, pp.447–448, April 1976.
[7] P. Wang, J. Xiao, and L. Ping, “Comparison of orthogonal and nonorthogonal approaches to future wireless cellular systems,” IEEE Veh. Technol. Mag., vol.1, no.3, pp.4–11, Sept. 2006.
[8] K. Higuchi and A. Benjebbour, “Non-orthogonal multiple access (NOMA) with successive interference cancellation for future radio access,” IEICE Trans. Commun., vol.E98-B, no.3, pp.403–414, March 2015.
[9] Z. Ding, Y. Liu, J. Choi, Q. Sun, M. Elkashlan, I. Chih-Lin, and H.V. Poor, “Application of non-orthogonal multiple access in LTE and 5G networks,” IEEE Commun. Mag., vol.55, no.2, pp.185–191, Feb. 2017.
[10] N. Otao, Y. Kishiyama, and K. Higuchi, “Performance of non-orthogonal multiple access with SIC in cellular downlink using proportional fair-based resource allocation,” IEICE Trans. Commun., vol.E98-B, no.2, pp.344–351, Feb. 2015.
[11] N. Nonaka, Y. Kishiyama, and K. Higuchi, “Non-orthogonal multiple access using intra-beam superposition coding and SIC in base station cooperative MIMO cellular downlink,” IEICE Trans. Commun., vol.E98-B, no.8, pp.1651–1659, Aug. 2015.
[12] K. Higuchi and Y. Kishiyama, “Non-orthogonal multiple access using intra-beam superposition coding and successive interference cancellation for cellular MIMO downlink,” IEICE Trans. Commun., vol.E98-B, no.9, pp.1888–1895, Sept. 2015.
[13] 3GPP TR36.859 (V13.0.0), “Study on downlink multiuser superposition transmission (MUST) for LTE (Release 13),” Dec. 2015.
[14] L. Ping, L. Liu, K. Wu, and W.K. Leung, “Interleave division multiple-access,” IEEE Trans. Wireless Commun., vol.5, no.4, pp.938–947, April 2006.
[15] Y. Hu, C. Xu, and L. Ping, “NOMA and IDMA in random access systems,” Proc. IEEE VTC2018-Spring, Porto, Portugal, June 2018.

[16] R. Hoshyar, F.P. Wathan, and R. Tafazolli, "Novel low-density signature for synchronous CDMA systems over AWGN channels," IEEE Trans. Signal Process., vol.56, no.4, pp.1616–1626, April 2008.
[17] H. Nikopour and H. Baligh, "Sparse code multiple access," Proc. IEEE PIMRC2013, London, UK, Sept. 2013.
[18] K. Au, L. Zhang, H. Nikopour, E. Yi, and A. Bayesteh, "Uplink contention based SCMA for 5G radio access," Proc. IEEE Globecom2014, Austin, USA, Dec. 2014.
[19] M. Kawata, K. Tateishi, and K. Higuchi, "Investigation on structure of interference canceller for IDMA-based random access," Proc. IEEE VTC2018-Fall, Chicago, U.S.A., Aug. 2018.
[20] P. Patel and J. Holtzman, "Performance comparison of a DS/CDMA system using a successive interference cancellation (IC) scheme and a parallel IC scheme under fading," Proc. IEEE ICC/SUPERCOMM'94, New Orleans, U.S.A., May 1994.
[21] M. Sawahashi, Y. Miki, H. Ando, and K. Higuchi, "Pilot symbol-assisted coherent multistage interference canceller using recursive channel estimation for DS-CDMA mobile radio," IEICE Trans. Commun., vol.E79-B, no.9, pp.1262–1270, Sept. 1996.
[22] K. Okawa, K. Higuchi, and M. Sawahashi, "Parallel-type coherent multi-stage interference canceller with iterative channel estimation using both pilot and decision-feedback date symbols for W-CDMA mobile radio," IEICE Trans. Commun., vol.E84-B, no.3, pp.446–456, March 2001.
[23] S. Sun, L.K. Rasmussen, H. Sugimoto, and T.J. Lim, "A hybrid interference canceller in CDMA," Proc. IEEE ISSSTA'98, Sun City, South Africa, Sept. 1998.
[24] D. Falconer, S.L. Ariyavisitakul, A. Benyamin-Seeyar, and B. Edison, "Frequency domain equalization for single-carrier broadband wireless systems," IEEE Commun. Mag., vol.40, no.4, pp.58–66, April 2002.
[25] 3GPP, TS 36.300, Evolved Universal Terrestrial Radio Access (E-UTRA) and Evolved Universal Terrestrial Radio Access Network (E-UTRAN); Overall description.
[26] M. Sabbaghian, D. Falconer, and H. Saeedi, "Comparison between convolutional and LDPC code-based turbo frequency domain equalization," Proc. IEEE Int. Conf. Commun., Istanbul, Turkey, June 2006.
[27] M. Sabbaghian and D.D. Falconer, "An analytical approach for finite block length performance analysis of turbo frequency-domain equalization," IEEE Trans. Veh. Technol., vol.58, no.3, pp.1292–1301, March 2009.
[28] C. Xu, L. Ping, P. Wang, S. Chan, and X. Lin, "Decentralized power control for random access with successive interference cancellation," IEEE J. Sel. Areas Commun., vol.31, no.11, pp.2387–2396, Nov. 2013.

Masayuki Kawata received the B.E. and M.E. degrees from Tokyo University of Science, Noda, Japan in 2018 and 2020, respectively. In 2020, he joined Fujitsu Limited.

Kiichi Tateishi received the B.S. and M.S. degrees from Tokyo University of Science in 2011 and 2013, respectively. Since he joined NTT DOCOMO in 2013, he has been involved in the research and development of 5G radio access technologies. From 2013 to 2018, he was in the 5G laboratory and engaged in 5G trials of multi-antenna technologies. Now, he is engaged in development and evaluations of 5G radio access network. He received the Young Researchers' Award from IEICE in 2017.

Kenichi Higuchi received the B.E. degree from Waseda University, Tokyo, Japan, in 1994, and received the Dr.Eng. degree from Tohoku University, Sendai, Japan in 2002. In 1994, he joined NTT Mobile Communications Network, Inc. (now, NTT DOCOMO, INC.). While with NTT DOCOMO, INC., he was engaged in the research and standardization of wireless access technologies for wideband DS-CDMA mobile radio, HSPA, LTE, and broadband wireless packet access technologies for systems beyond IMT-2000. In 2007, he joined the faculty of the Tokyo University of Science and currently holds the position of Professor. His current research interests are in the areas of wireless technologies and mobile communication systems, including advanced multiple access, radio resource allocation, inter-cell interference coordination, multiple-antenna transmission techniques, signal processing such as interference cancellation and turbo equalization, and issues related to heterogeneous networks using small cells. He was a co-recipient of the Best Paper Award of the International Symposium on Wireless Personal Multimedia Communications in 2004 and 2007, a recipient of the Young Researcher's Award from the IEICE in 2003, the 5th YRP Award in 2007, the Prime Minister Invention Prize in 2010, and the Invention Prize of Commissioner of the Japan Patent Office in 2015. He is a member of the IEEE.